Journal of Geophysical Research: Atmospheres

Supporting Information for

Airborne measurements of western U.S. wildfire emissions: Comparison with prescribed burning and air quality implications

Xiaoxi Liu[1], L. Gregory Huey[1], Robert J. Yokelson[2], Vanessa Selimovic[2], Isobel J. Simpson[3], Markus Müller[2,4], Jose L. Jimenez[5,6], Pedro Campuzano-Jost[5,6], Andreas J. Beyersdorf[7,*], Donald R. Blake[3], Zachary Butterfield[8,†], Yonghoon Choi[7,9], John D. Crounse[10], Douglas A. Day[5,6], Glenn S. Diskin[7], Manvendra K. Dubey[8], Edward Fortner[11], Thomas F. Hanisco[12], Weiwei Hu[5,6], Laura E. King[1], Lawrence Kleinman[13], Simone Meinardi[3], Tomas Mikoviny[14], Timothy B. Onasch[11], Brett B. Palm[5,6], Jeff Peischl[5,15], Ilana B. Pollack[5,15,§], Thomas B. Ryerson[15], Glen W. Sachse[7], Arthur J. Sedlacek[13], John E. Shilling[16], Stephen Springston[13], Jason M. St. Clair[10,‡], David J. Tanner[1], Alexander P. Teng[10], Paul O. Wennberg[10,17], Armin Wisthaler[4,14], and Glenn M. Wolfe[12,18]

[1]School of Earth and Atmospheric Sciences, Georgia Institute of Technology, Atlanta, Georgia, USA
[2]Department of Chemistry, University of Montana, Missoula, Montana, USA
[3]Department of Chemistry, University of California, Irvine, California, USA
[4]Institute for Ion Physics and Applied Physics, University of Innsbruck, Innsbruck, Austria
[5]Cooperative Institute for Research in Environmental Sciences (CIRES), University of Colorado Boulder, Boulder, Colorado, USA
[6]Department of Chemistry and Biochemistry, University of Colorado at Boulder, Boulder, Colorado, USA
[7]NASA Langley Research Center, Hampton, Virginia, USA
[8]Earth and Environmental Sciences Division, Los Alamos National Laboratory, Los Alamos, New Mexico, USA
[9]Science Systems and Applications, Inc., Hampton, Virginia, USA
[10]Division of Geological and Planetary Sciences, California Institute of Technology, Pasadena, California, USA
[11]Aerodyne Research Inc., Billerica, Massachusetts, USA
[12]Atmospheric Chemistry and Dynamics Laboratory, NASA Goddard Space Flight Center, Greenbelt, Maryland, USA
[13]Environmental and Climate Sciences Department, Brookhaven National Laboratory, Upton, New York, USA
[14]Department of Chemistry, University of Oslo, Oslo, Norway
[15]Earth System Research Laboratory, National Oceanic and Atmospheric Administration, Boulder, Colorado, USA
[16]Atmospheric Sciences and Global Change Division, Pacific Northwest National Laboratory, Richland, Washington, USA
[17]Division of Engineering and Applied Science, California Institute of Technology, Pasadena,

California, USA
[18]Joint Center for Earth Systems Technology, University of Maryland Baltimore County, Baltimore, Maryland, USA
[*]now at: Department of Chemistry, California State University, San Bernardino, California, USA
[†]now at: Department of Atmospheric, Oceanic, and Space Sciences, University of Michigan, Ann Arbor, Michigan, USA
[‡]now at: Atmospheric Chemistry and Dynamics Laboratory, NASA Goddard Space Flight Center, Greenbelt, Maryland, USA and Joint Center for Earth Systems Technology, University of Maryland Baltimore County, Baltimore, Maryland, USA
[§]now at: Department of Atmospheric Science, Colorado State University, Fort Collins, Colorado, USA

Contents of this file

Text S1
Figure S1-S4

Introduction

The supporting information contains:

- A validation of AMS measurements in the Rim Fire plumes.
- Four figures: (S1) Comparison of AMS measurements with aerosol volume and extinction at 532 nm measurements [*Wang et al.*, 2010] in the Rim Fire plumes; (S2) LAS aerosol volume size distributions measured in the Rim Fire plumes; (S3) examples of time series in fire plumes; and (S4) emission factors (EFs) as a function of modified combustion efficiency (MCE) for gaseous species with slopes not significantly different from zero.

Text S1. Validation of AMS measurements in the Rim Fire plumes

During SEAC^{4}RS, the collection efficiency (CE) of the Aerodyne High-Resolution Time-of-Flight Aerosol Mass Spectrometer (hereinafter AMS) was calculated based on the composition-dependent algorithm of *Middlebrook et al.* [2012] using 1 min averaging. The average CE for the Western biomass burning (BB) plumes during the SEAC^{4}RS campaign was estimated to be 0.5 by this method. We also used a CE of 0.5 for BBOP fire plumes, during which no reliable particle size measurement is available for such a comparison. In order to validate the AMS quantification for the SEAC^{4}RS plumes, we converted the mass concentrations of measured non-refractory components to volume assuming an internally mixed aerosol and literature densities for each species [*DeCarlo et al.*, 2004; *Salcedo et al.*, 2006], with the OA density estimated based on the method of *Kuwata et al.* [2012]. It was then compared with the aerosol volume calculated from measurements by a laser aerosol spectrometer (LAS; TSI Inc., St. Paul, MN). The LAS was calibrated with PSLs (n_D=1.595) and the reported diameters were corrected by a factor of 1.115 to account for the lower refractive index of ambient particles during SEAC^{4}RS (n_D=1.52-1.54) [*Shingler et al.*, 2016]. The correction factor is based on the relative response of a collocated ultra-high sensitivity aerosol spectrometer (UHSAS; Droplet Measurements Technologies, Boulder, CO) to both PSLs and Ammonium Sulfate particles (n_D=1.53 [*Zarzana et al.*, 2014]) . Figure S1 shows the volume comparison with orthogonal distance regression lines. The slopes for wildfire plumes and non-BB air masses are 0.82 and 1.21, respectively, both of which are within the combined measurement uncertainties. These results support that the AMS was certainly not overestimating the mass concentration in BB plumes, which would have been the case if CE was substantially higher than 0.5. For the BB plumes, a clear non-linear trend in LAS response is observed above 50 ug sm^{-3}, which is due to undercounting of the LAS at high particle counts, a well-known drawback of this technique.

An alternative way to check the AMS quantification is by estimating the mass extinction efficiency (MEE) using two different methods. The first method uses a linear regression of total extinction at 532 nm (sum of scattering from a TSI Mod 3563 nephelometer, St Paul, MI) plus absorption from a Radiance Research particle soot absorption photometer (Shoreview, WA), with absorption being <5% of the total) versus the total mass of AMS species, as shown in the right side of Figure S1. The slopes are 6.83±0.16 $m^2 g^{-1}$ for all Rim Fire plumes and 5.68±0.13 $m^2 g^{-1}$ for aged Rim Fire plumes. In non-BB air masses, the slope is 6.69±0.07 $m^2 g^{-1}$. These are within the range of typical values (2-10 $m^2 g^{-1}$) that have been observed in the field [*Hand and Malm*, 2007; *DeCarlo et al.*, 2008; *Dunlea et al.*, 2009; *Shinozuka et al.*, 2009]. Figure S2 shows the aerosol volume size distributions measured in fresh and aged Rim Fire plumes by the LAS. The volume size distributions peaked at 315 nm and 330 nm in the fresh and aged plumes, respectively. Using these size distributions and the refractive indices reported by *Shingler et al.* [2016], we calculated mass scattering efficiency (MSE) based on Mie scattering code [*Bohren and Huffman*, 1983]. The MSEs are 7.9 $m^2 g^{-1}$ and 6.9 $m^2 g^{-1}$ for fresh and aged Rim Fire plumes. As scattering accounted for most of (>90%) the total extinction, a reasonable agreement between the calculated MSE and the MEE derived from regression slopes within the combined uncertainties of both measurements thus further validates the AMS measurements. As for the previous comparison, the slightly higher values obtained with the second method confirm that the mass concentrations reported by the AMS in the fire plumes are not overestimated.

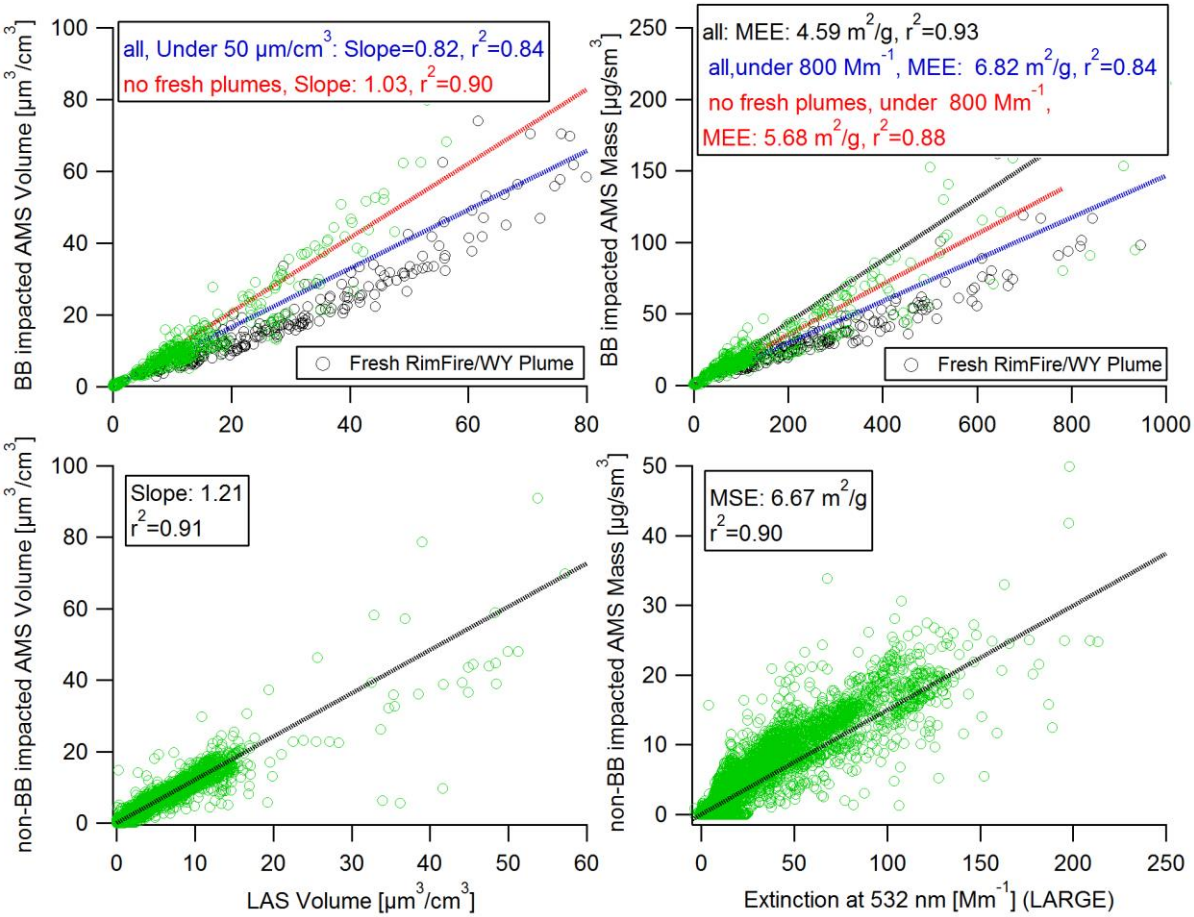

Figure S1. Comparison for the SEAC^{4}RS campaign of estimated aerosol volumes from AMS and LAS measurements (left) and AMS total mass with dry aerosol PM_1 extinction at 532 nm, as calculated from the sum of dry scattering (TSI nephelometer) and absorption (Radiance Research PSAP) (right). The bottom two figures show data for the PBL over continental North America in the absence of major BB influence, while the top two plots summarize all the large BB plumes encountered during SEAC^{4}RS (except for agricultural fires). The slopes are obtained by orthogonal distance regression with the intercepts fixed to 0, which is justified since the zeros of all instruments are checked frequently (and corrected, if needed) by measuring through filters.

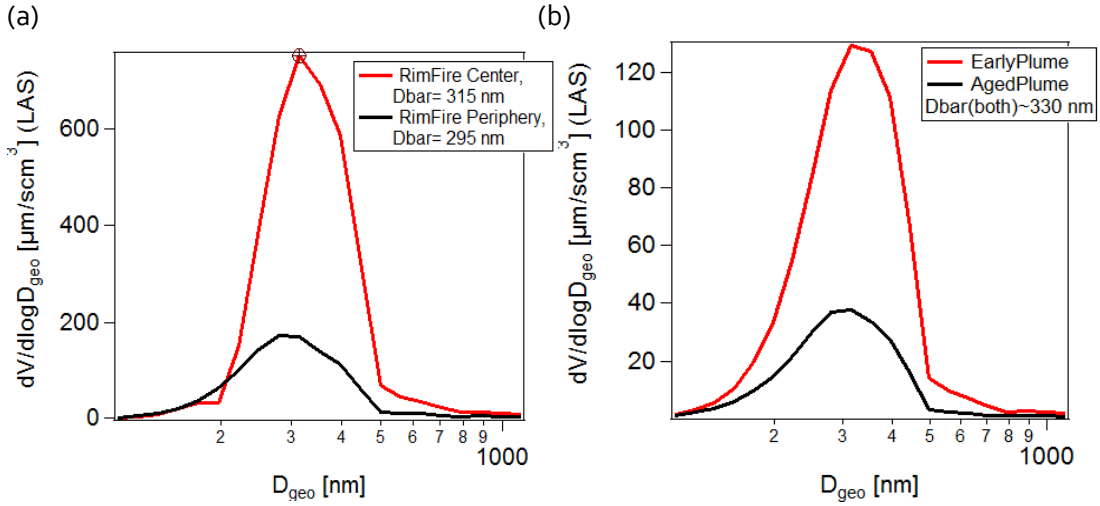

Figure S2. Averaged LAS aerosol volume size distributions measured in the Rim Fire plumes: (a) fresh plumes and (b) aged (1-2 days of transport) plumes. Optical diameters and volumes were corrected for refractive index (see text).

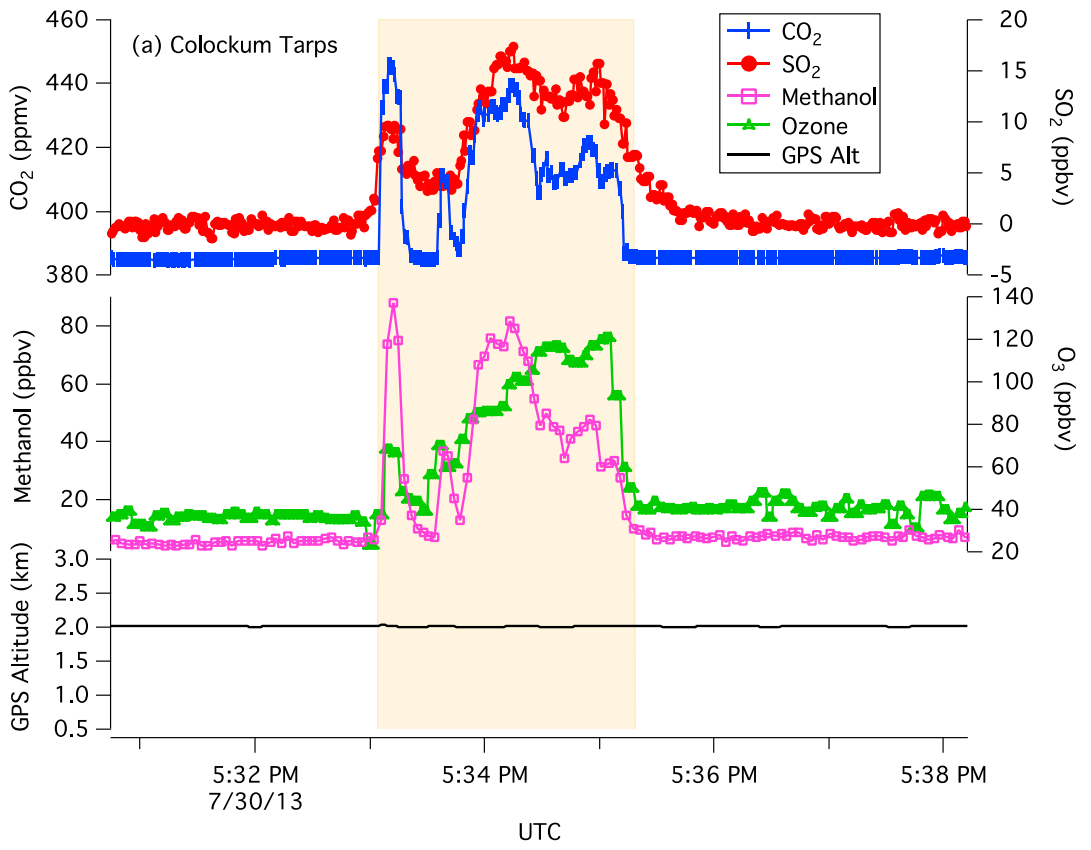
(a) Colockum Tarps
CO2
SO2
Methanol
Ozone
GPS Alt
CO2 (ppmv)
SO2 (ppbv)
Methanol (ppbv)
O3 (ppbv)
GPS Altitude (km)
5:32 PM
7/30/13
5:34 PM
5:36 PM
5:38 PM
UTC

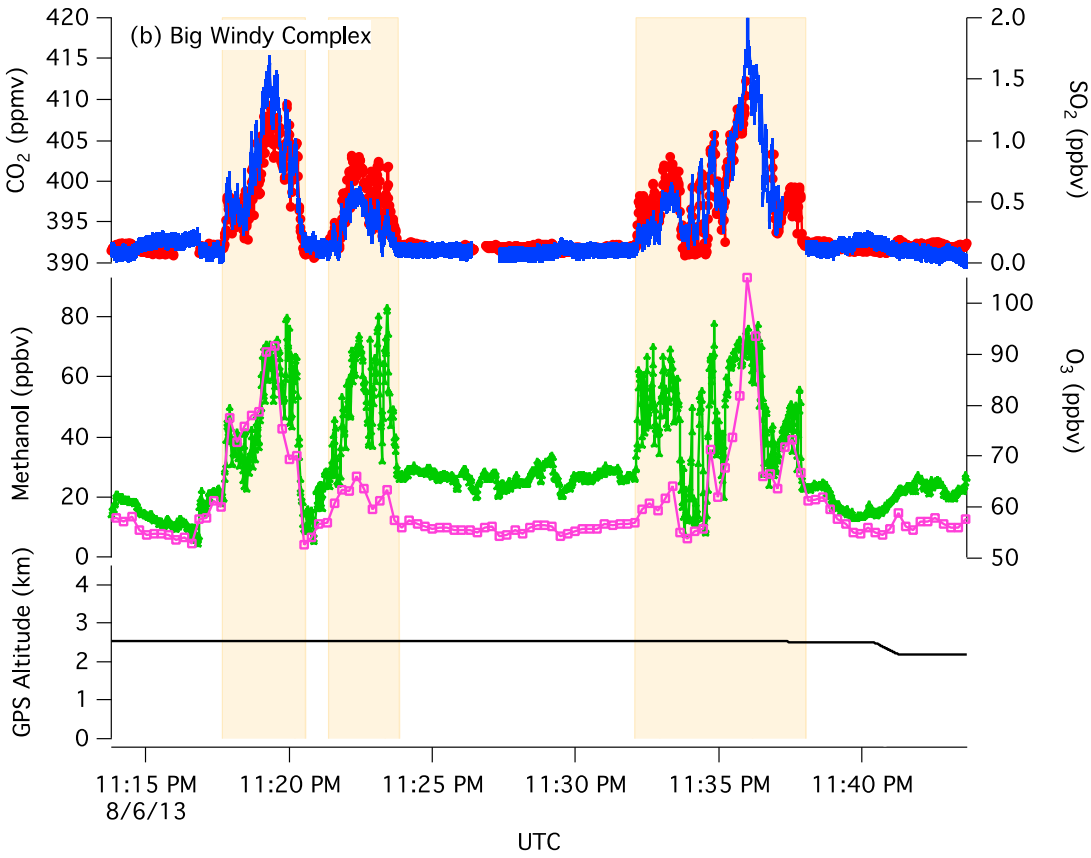
(b) Big Windy Complex
CO2 (ppmv)
SO2 (ppbv)
Methanol (ppbv)
O3 (ppbv)
GPS Altitude (km)
11:15 PM
8/6/13
11:20 PM
11:25 PM
11:30 PM
11:35 PM
11:40 PM
UTC

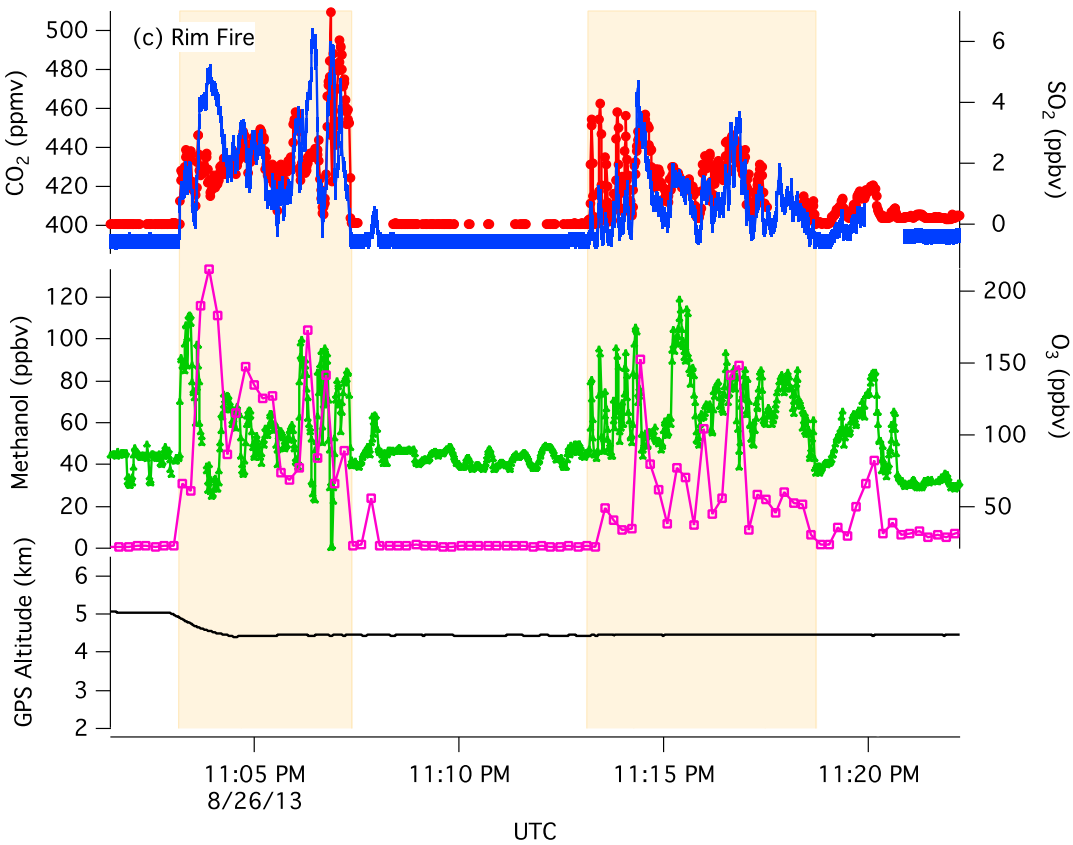

Figure S3. Examples of time series of CO_2, SO_2, methanol, O_3, and GPS altitude for: (a) Colockum Tarps; (b) Big Windy Complex; and (c) Rim Fire. Shaded area shows the duration of fresh plume used for analysis.

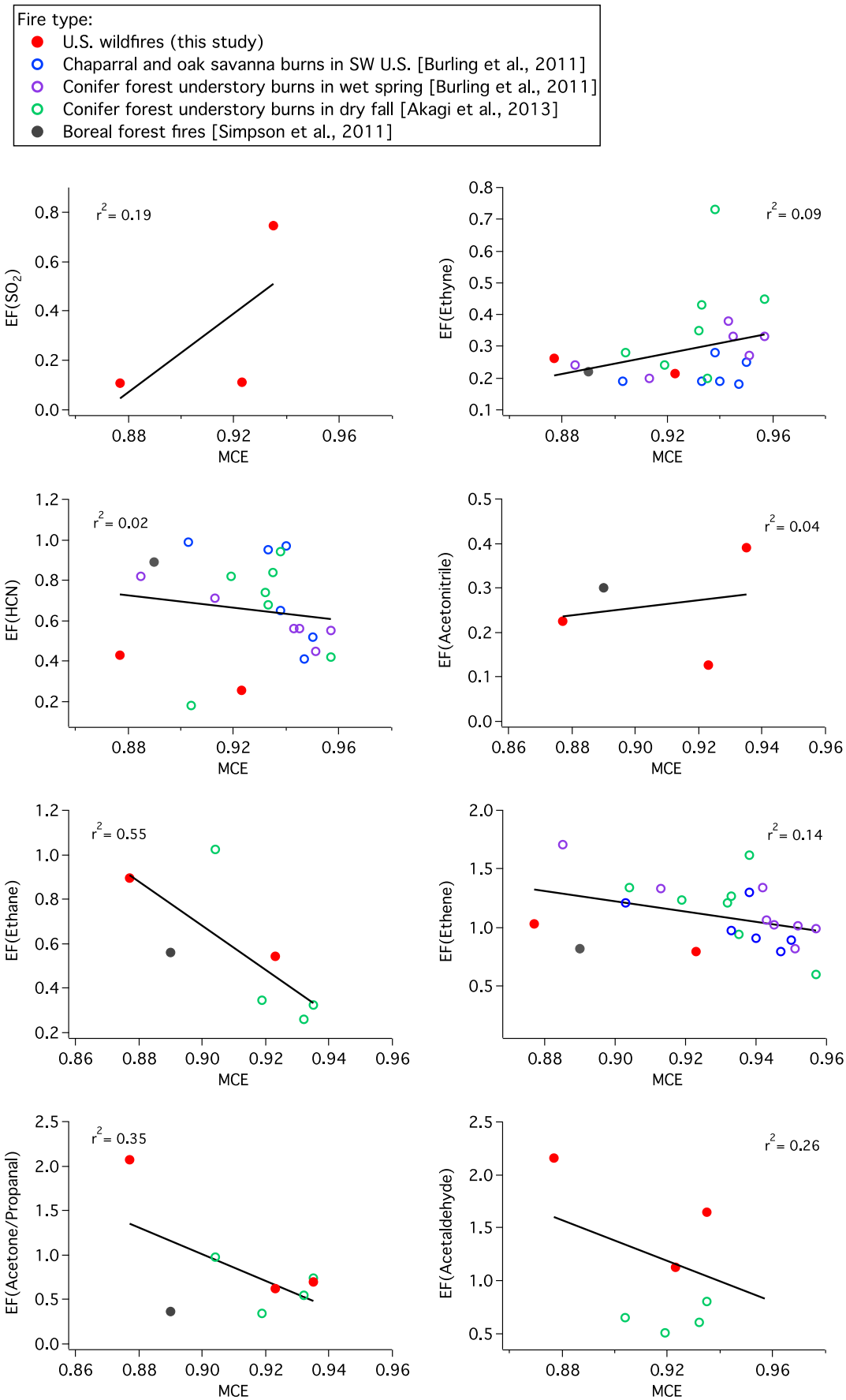
Fire type:
U.S. wildfires (this study)
Chaparral and oak savanna burns in SW U.S. [Burling et al., 2011]
Conifer forest understory burns in wet spring [Burling et al., 2011]
Conifer forest understory burns in dry fall [Akagi et al., 2013]
Boreal forest fires [Simpson et al., 2011]
EF(SO2)
r2 = 0.19
EF(Ethyne)
r2 = 0.09
EF(HCN)
r2 = 0.02
EF(Acetonitrile)
r2 = 0.04
EF(Ethane)
r2 = 0.55
EF(Ethene)
r2 = 0.14
EF(Acetone/Propanal)
r2 = 0.35
EF(Acetaldehyde)
r2 = 0.26
MCE

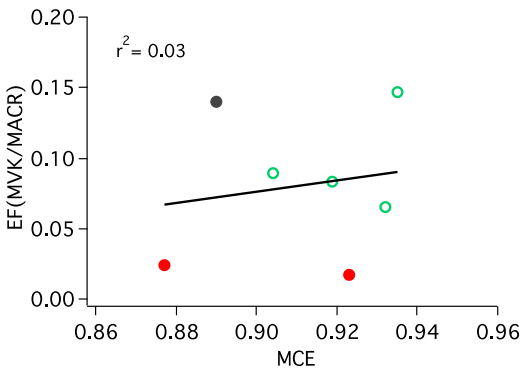

Figure S4. Emission factors (g kg^{-1}) of gaseous species as a function of MCE for the three wildfires of this study, the boreal forest fires of *Simpson et al.* [2011], and the prescribed fires of *Burling et al.* [2011] and *Akagi et al.* [2013]. Gases shown here are associated with slopes that are not significantly different from zero. Correlation coefficients (r^2) were derived from bivariate linear regressions of all plotted data.

Reference

Akagi, S. K., et al. (2013), Measurements of reactive trace gases and variable O_3 formation rates in some South Carolina biomass burning plumes, *Atmos. Chem. Phys.*, *13*(3), 1141-1165, doi: 10.5194/acp-13-1141-2013.

Bohren, C. F., and D. R. Huffman (1983), *Absorption and Scattering of Light by Small Particles*, John Wiley & Sons, New York, NY.

Burling, I. R., R. J. Yokelson, S. K. Akagi, S. P. Urbanski, C. E. Wold, D. W. T. Griffith, T. J. Johnson, J. Reardon, and D. R. Weise (2011), Airborne and ground-based measurements of the trace gases and particles emitted by prescribed fires in the United States, *Atmos. Chem. Phys.*, *11*(23), 12197-12216, doi: 10.5194/acp-11-12197-2011.

DeCarlo, P. F., J. G. Slowik, D. R. Worsnop, P. Davidovits, and J. L. Jimenez (2004), Particle Morphology and Density Characterization by Combined Mobility and Aerodynamic Diameter Measurements. Part 1: Theory, *Aerosol Sci. Tech.*, *38*(12), 1185-1205, doi: 10.1080/027868290903907.

DeCarlo, P. F., et al. (2008), Fast airborne aerosol size and chemistry measurements above Mexico City and Central Mexico during the MILAGRO campaign, *Atmos. Chem. Phys.*, *8*(14), 4027-4048, doi: 10.5194/acp-8-4027-2008.

Dunlea, E. J., et al. (2009), Evolution of Asian aerosols during transpacific transport in INTEX-B, *Atmos. Chem. Phys.*, *9*(19), 7257-7287, doi: 10.5194/acp-9-7257-2009.

Hand, J. L., and W. C. Malm (2007), Review of aerosol mass scattering efficiencies from ground-based measurements since 1990, *J. Geophys. Res. Atmos.*, *112*(D16), doi: 10.1029/2007JD008484.

Kuwata, M., S. R. Zorn, and S. T. Martin (2012), Using Elemental Ratios to Predict the Density of Organic Material Composed of Carbon, Hydrogen, and Oxygen, *Environ. Sci. Technol.*, *46*(2), 787-794, doi: 10.1021/es202525q.

Middlebrook, A. M., R. Bahreini, J. L. Jimenez, and M. R. Canagaratna (2012), Evaluation of Composition-Dependent Collection Efficiencies for the Aerodyne Aerosol Mass Spectrometer using Field Data, *Aerosol Sci. Tech.*, *46*(3), 258-271, doi: 10.1080/02786826.2011.620041.

Salcedo, D., et al. (2006), Characterization of ambient aerosols in Mexico City during the MCMA-2003 campaign with Aerosol Mass Spectrometry: results from the CENICA Supersite, *Atmos. Chem. Phys.*, *6*(4), 925-946, doi: 10.5194/acp-6-925-2006.

Shingler, T., et al. (2016), Airborne characterization of subsaturated aerosol hygroscopicity and dry refractive index from the surface to 6.5 km during the SEAC^{4}RS campaign, *J. Geophys. Res. Atmos.*, *121*(8), 4188-4210, doi: 10.1002/2015JD024498.

Shinozuka, Y., et al. (2009), Aerosol optical properties relevant to regional remote sensing of CCN activity and links to their organic mass fraction: airborne observations over Central Mexico and the US West Coast during MILAGRO/INTEX-B, *Atmos. Chem. Phys.*, *9*(18), 6727-6742, doi: 10.5194/acp-9-6727-2009.

Simpson, I. J., et al. (2011), Boreal forest fire emissions in fresh Canadian smoke plumes: C_1-C_{10} volatile organic compounds (VOCs), CO_2, CO, NO_2, NO, HCN and CH_3CN, *Atmos. Chem. Phys.*, *11*(13), 6445-6463, doi: 10.5194/acp-11-6445-2011.

Wang, Z., et al. (2010), The Dynamic Shape Factor of Sodium Chloride Nanoparticles as Regulated by Drying Rate, *Aerosol Sci. Tech.*, *44*(11), 939-953, doi: 10.1080/02786826.2010.503204.

Zarzana, K. J., C. D. Cappa, and M. A. Tolbert (2014), Sensitivity of Aerosol Refractive Index Retrievals Using Optical Spectroscopy, *Aerosol Sci. Tech.*, *48*(11), 1133-1144, doi: 10.1080/02786826.2014.963498.